Exploring structures, electronic and reactivity properties of Au6Hn (n = 1–12) clusters: A DFT approach

ARTICLE *in* COMPUTATIONAL AND THEORETICAL CHEMISTRY · DECEMBER 2012

Impact Factor: 1.55 · DOI: 10.1016/j.comptc.2012.09.006

2 AUTHORS:

Subhi Baishya
Tezpur University
4 PUBLICATIONS **10** CITATIONS
SEE PROFILE

Ramesh C Deka
Tezpur University
99 PUBLICATIONS **1,007** CITATIONS
SEE PROFILE

Computational and Theoretical Chemistry 1002 (2012) 1–8

Contents lists available at SciVerse ScienceDirect

Computational and Theoretical Chemistry

journal homepage: www.elsevier.com/locate/comptc

Exploring structures, electronic and reactivity properties of Au_6H_n (n = 1–12) clusters: A DFT approach

Subhi Baishya, Ramesh C. Deka *

Department of Chemical Sciences, Tezpur University, Napaam 784 028, Tezpur, Assam, India

ARTICLE INFO

Article history:
Received 26 April 2012
Received in revised form 14 August 2012
Accepted 6 September 2012
Available online 28 September 2012

Keywords:
Density Functional Theory
Generalized gradient approximation
Hydrogen adsorbed gold hexamer
Fukui functions

ABSTRACT

Density functional calculations at the PBE/DNP level have been carried out to investigate the structures, electronic and reactivity properties of Au_6H_n (n = 1–12) clusters. Adsorption of hydrogen atoms stabilizes the Au_6 cluster indicated by the high binding energies. The adsorption of H atoms till Au_6H_6 retains the planar triangular structure of Au_6. However, the triangular structure is distorted on further addition of H atoms till Au_6H_9. In clusters Au_6H_{10}, Au_6H_{11} and Au_6H_{12}, though the triangular structure is restored but the structures are non-planar. The averaged Hirshfeld atomic charges indicate the H atoms to be negatively charged in all the clusters. Odd–even alternation in HOMO–LUMO gap, chemical hardness, vertical ionization potential, adiabatic ionization potential and binding energy is observed with the clusters having even number of H atoms possessing higher values and are observed to be more stable than their congeners with odd number of H atoms. DFT based reactivity descriptors indicate that in Au_6, the Au atoms forming the vertices of the outer triangle have higher relative electrophilicity value while those forming the vertices of the inner triangle have higher relative nucleophilicity value. However, in Au_6H_6, two nearby Au sites forming the vertices of the inner and outer triangle have the highest relative electrophilicity and relative nucleophilicity values. In Au_6H_{12}, these are located in the inner triangle.

1. Introduction

Bulk gold is noble; however, when the size is reduced to nanometer range, it exhibits striking reactive behavior [1–4]. A number of both experimental [5–11] and theoretical [12–31] methods have been made on gold nanoparticles and clusters that possess unique physical and chemical properties. The potential application of gold nanoparticles and clusters as building blocks for functional nanostructured materials, electronic devices and nanocatalysts [32–35] has motivated the recent surge of research activity in the area of their physical and chemical properties.

Gold with a singly filled s-shell with an atomic configuration [Xe] $4f^{14}$ $5d^{10}$ $6s^1$ exhibits properties similar to alkali metals. However, it possess significant relativistic effect which is larger than any other element with $Z < 100$ in the periodic table. Presence of relativistic effect reduces the s–d energy gap thus inducing hybridization of the atomic 5d–6s energy levels and causing an overlap of the 5d shells of the neighboring atoms in the cluster [36]. For instance, presence of relativistic effect has led to the uniqueness of gold in having stable planar 2D clusters up to n = 12 [37,38].

Hydrogen has an atomic configuration of $1s^1$ similar to gold that makes it interesting to study the interaction of small gold clusters with hydrogen atoms, both H and Au having single valence s electron. Gold hydrides have attracted considerable attention as they serve as important intermediates in gold catalyzed reactions [39,40] such as hydrogenation [41], hydrosilylation [42], C–H bond activation [43], and aerobic oxidation of alcohols [44]. The study of gold hydride clusters is important to understand the adsorption of hydrogen onto metal surfaces. Moreover, the gold hydrides serve as archetype to study the relativistic effects. The chemistry of gold has been demonstrated by several theoretical and experimental works [45,46] to have significant resemblance to that of the hydrogen atom. In 1978, *ab initio* studies were performed by Hay et al. [47] on diatomic gold hydride using relativistic effective core potentials. A number of experimental and theoretical studies have been reported about the interaction of the gold clusters with hydrogen [48–51]. Phala performed DFT calculation to study the interaction of small Au_n (n = 1–13) clusters with H and CO [52]. Buckart et al. [46] in 2003 presented that the spectra of Au_n^- and $Au_{n-1}H^-$ showed identical features for $n > 2$ in their photoelectron spectra; thus suggesting that hydrogen behaved as protonated species. Even though a large number of studies have been done on gold cluster hydrides involving a single hydrogen atom, but a very rare amount of study has been done on multi-hydrogen atom interaction [53]. Apart from the interaction between hydrogen and gold cluster, insight into the reactivity of Au cluster and the reacting sites within them is also important. The ability to withdraw (electrophilicity) or donate (nucleophilicity) electrons of the various sites in a cluster is closely related to its catalytic activ-

* Corresponding author. Tel.: +91 3712 267008; fax: +91 3712 267005.
E-mail address: ramesh@tezu.ernet.in (R.C. Deka).

2210-271X/$ - see front matter © 2012 Elsevier B.V. All rights reserved.
http://dx.doi.org/10.1016/j.comptc.2012.09.006

ity. However, exploring the reactive sites in hydrogen adsorbed gold clusters is still lacking behind.

A planar triangular structure with D_{3h} symmetry has been assigned to Au_6 [54]. Based on this structure, we aim to study multi-hydrogen adsorption on Au_6 and try to reveal the

(i) structure and stability of Au_6H_n (n = 1–12) clusters,
(ii) electronic and reactivity properties of the Au_6H_n clusters.

The paper is outlined as follows. Section 2 summarizes the computational methods. The following section (Section 3) shows the results obtained from the calculations. Finally, Section 4 gives the summary of the present study.

2. Computational methods

Density Functional Theory (DFT) calculations are carried out using DMol^3 [55] package utilizing PBE functional [56] incorporating the Perdew, Burke, Ernzerhof correlation at the generalized gradient approximation (GGA) level. The DNP numerical basis set is the highest quality set available in DMol^3 and has been chosen for our calculations. DNP basis functions are the double numerical sets containing a polarization d-function on heavy atoms and polarization p-function on hydrogen. Although the size is comparable to 6-31G** basis set but the numerical basis set of given size are much more accurate than Gaussian basis set of same size. Relativistic calculations in gold are important and are performed with scalar relativistic corrections to valence orbitals relevant to atomic bonding properties via a local pseudopotential (VPSR) [57]. For matrix integrations fine grid mesh points are employed. Convergence criterion of 10^{-6} a.u. has been used for self consistent field procedures on energy and electron density. To justify the level of calculation employed in the present work, we have compared the calculated values of bond length (R_e), dissociation energy (D_e) and vibrational frequency (ω_e) of Au_2 at different levels of theory (VWN, BLYP, PW91, PBE functional and DNP basis set) with the experimental values (Table 1).

The stability and the electronic properties of the clusters have been determined from the binding energy per atom, binding energy per H-atom, the vertical ionization potential and the chemical hardness values. For a given cluster, the binding energy is a measure of its thermodynamic stability. We calculate the average binding energies using the following formulas:

$$E_b = [6E(\mathrm{Au}) + nE(\mathrm{H}) - E(\mathrm{Au_6H_n})]/(n+6) \quad (1)$$

$$E_b^a = [E(\mathrm{Au_6}) + nE(\mathrm{H}) - E(\mathrm{Au_6H_n})]/(n) \quad (2)$$

where E_b is the binding energy per atom, E_b^a is the binding energy per H-atom, E(Au) and E(H) are the energies of Au and H atoms respectively, $E(Au_6)$ and $E(Au_6H_n)$ are the energies of Au_6 and Au_6H_n clusters respectively and n is the number of H atoms in a given cluster.

Table 1
Comparison of the performance of different functional for bond length (Å), dissociation energy (eV) and vibrational frequency (cm^{-1}) of Au_2 with the experimental values. The basis set used for the calculations is the DNP basis set.

System	Property	Experimental	Method
Au_2	R_e (Å)	2.47	2.44 (VWN)
			2.53 (BLYP)
			2.49 (PW91)
			2.49 (PBE)
	D_e (eV)	2.30	2.97 (VWN)
			2.14 (BLYP)
			2.43 (PW91)
			2.40 (PBE)
	ω_e (cm^{-1})	191	169.6 (BLYP)
			184.0 (PBE)

The vertical ionization potential (VIP) is calculated as:

$$\mathrm{VIP} = E(\mathrm{Au_6H_n})^+ - E(\mathrm{Au_6H_n}) \quad (3)$$

where $E(Au_6H_n)^+$ is the energy of the cationic cluster at the optimized geometry of the neutral cluster. Generally, larger vertical ionization potential implies deeper HOMO energy level leading to lesser reactivity or higher chemical stability.

A useful parameter for examining the kinetic stability of the clusters is the HOMO–LUMO gap (HLG).

$$\mathrm{HLG} = E(\mathrm{LUMO}) - E(\mathrm{HOMO}) \quad (4)$$

Larger HOMO–LUMO gap corresponds to higher energy for perturbing the electronic structure thus indicating higher stability of electronic structure.

The reactivity of a system can be described in terms of its chemical hardness. The second derivative of energy (E) with respect to the number of electrons (N) at constant external potential, $v(\vec{r})$ defines hardness, η.

$$\eta = 1/2(\partial^2 E/\partial N^2)_{v(\vec{r})} = 1/2(\partial\mu/\partial N)_{v(\vec{r})} \quad (5)$$

where μ is the chemical potential of the system.

Applying three point finite difference approximation, hardness can be approximated as:

$$\eta = (IP - EA)/2 \quad (6)$$

where IP is the ionization potential and EA is the electron affinity of the system.

Within the framework of Density Functional Theory, applying Koopmans approximation, hardness can be expressed as:

$$\eta = (E_{\mathrm{LUMO}} - E_{\mathrm{HOMO}})/2 \quad (7)$$

Condensed Fukui functions in a finite difference approximation have been proposed by Yang et al. [58] to describe the site reactivity or site selectivity and are given as:

$$f^+ = q(N+1) - q(N); \quad \text{for nucleophilic attack} \quad (8a)$$

$$f^- = q(N) - q(N-1); \quad \text{for electrophilic attack} \quad (8b)$$

$$f^0 = 1/2[q(N+1) - q(N-1)]; \quad \text{for radical attack} \quad (8c)$$

$q(N)$, $q(N+1)$, $q(N-1)$ are the electronic populations for atoms with (N), ($N+1$) and ($N-1$) electrons respectively.

Roy et al. [59] proposed relative nucleophilicity as:

$$f_{\mathrm{nu}} = f^-/f^+ \quad (9a)$$

and relative electrophilicity as:

$$f_{\mathrm{ele}} = f^+/f^- \quad (9b)$$

These are useful to identify the reactive site at which the reaction shall take place. Within the same molecule $f_{\mathrm{nu}}/f_{\mathrm{ele}}$ is important to compare the reactivity. For a site, if $f_{\mathrm{nu}} \gg f_{\mathrm{ele}}$, then the site is favorable for an electrophilic attack and favorable for nucleophilic attack if $f_{\mathrm{ele}} \gg f_{\mathrm{nu}}$. A site for which f_{nu} is almost equal to f_{ele} is said to be an amphiphilic site.

3. Results and discussion

3.1. Geometric structure and electronic properties

The planar triangular structure with D_{3h} symmetry for Au_6 cluster has been concluded to be the lowest energy structure from our previous work [54] and the present work utilizes this stable

structure (Fig. 1a) for further calculations. Based on the optimized lowest energy structure of Au_6 cluster, we perform an extensive minimum energy structural search for a number of hydrogen atoms binding to the Au_6 cluster. The lowest energy structures for Au_6H_n (n = 1–12) are shown in Fig. 1b–m. The other higher energy isomers obtained during the structural search are shown in

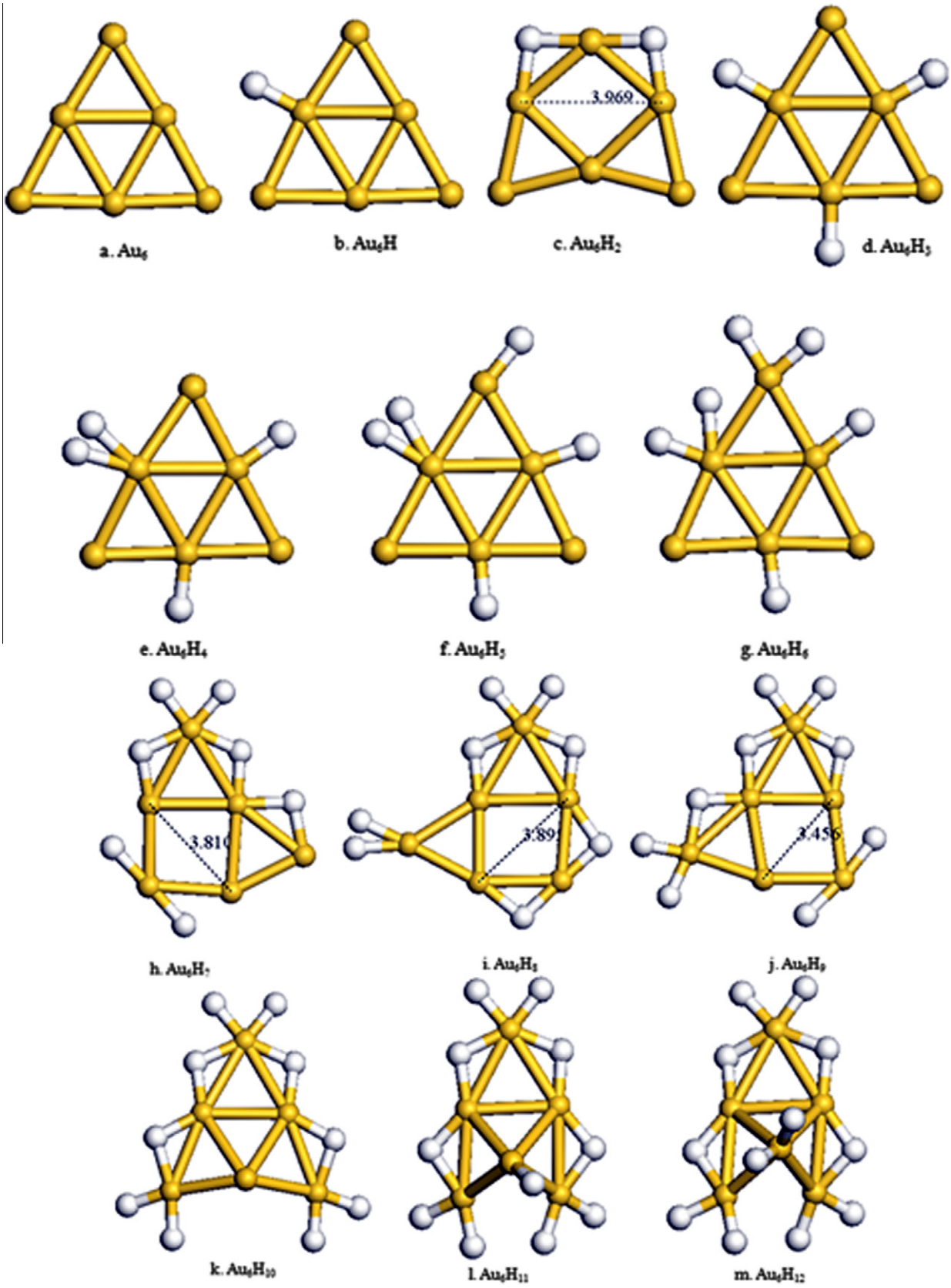

Fig. 1. (a–m) Optimized structures of the pure Au_6 cluster and the Au_6H_n (n = 1–12) clusters from PBE/DNP level of calculation.

Fig. S1 and their total and relative energies are summarized in Table S1 of the Supporting information. Absence of negative vibrational frequencies indicates the lowest energy optimized structures to be the minima rather than transition states. For all the clusters, Au_6H_n (n = 1–12) both the low spin and high spin states have been considered. The low spin singlet and doublet states are found to be lower in energy compared to the high spin triplet and quartet states for clusters with even and odd number of H-atoms, respectively. The energies of all the clusters in both low spin and high spin states are tabulated in Table S2 of the Supporting information. Thus, the clusters are stable in the low spin state irrespective of the number of H-atoms.

Adsorption of the first H atom on the Au_6 cluster was considered in three different sites-outer Au atom, inner Au atom and in the bridge position. It has been found that the Au_6H cluster with H atom adsorbed on the outer Au atom is 6.30 kJ/mol higher in energy than the cluster with the H atom adsorbed on the inner Au atom. When the bridge position is considered, the H atom preferentially adsorbs in the inner Au atom rather than being bridged bonded in the optimized structure. The optimized structures of the Au_6H cluster with H atom adsorbed on outer Au atom and in the bridge position are shown in Fig. S2 of the Supporting information. When the addition of the second H atom was considered on three sites viz. an outer Au atom, Au atom with adsorbed H atom and an inner Au atom; the later was found to be more stable as compared to the H addition on an outer Au and the Au atom with adsorbed H atom. These were found to be 108.96 kJ/mol higher in energy than the Au_6H_2 cluster obtained from the adsorption of the H atom to an inner Au atom. Preferential adsorption of H atom on the inner Au atom can be correlated with the relative nucleophilicity (f^-/f^+) values. The inner Au atoms possess higher f^-/f^+ value and preference for it by the H atom indicates that H atom is likely to behave as an electrophile. It can be seen from Fig. 1 that the clusters, Au_6H_n (n = 1–6) are planar without any distortion in the triangular structure of Au_6. The H atoms bind in a head-on fashion to the Au atoms with the shortest Au–H bond length being 1.52–1.57 Å which can be compared with the experimental Au–H bond length of 1.52 Å in AuH. However, in Au_6H_2, the H atoms are bridge bonded between the inner Au atoms and the nearby outer Au atom with bond length of 1.73 Å. The average bond length of outer Au–Au bond increases from 2.59 Å in Au_6 to 2.62 Å in Au_6H_6 while the inner Au–Au bond length of 2.73 Å remains unchanged. However, in case of Au_6H_2, where the triangular structure is distorted, one of the inner Au–Au bonds (dotted bond, Fig. 1) is considerably elongated to 3.97 Å. Elongation of Au–Au bond indicates that the binding of H atoms on the Au_6 cluster is made at the cost of metal–metal bond weakening. Zhai et al. [60] reported Au–H bond length of 1.72 Å and Au–Au distance of 3.44 Å in Au_2H^- comparable with abnormally long Au–Au distance (3.6 Å) observed in gold nanowires. On further addition of an H atom to the Au_6H_6 cluster that results in the Au_6H_7, the triangular structure of Au_6 is considerably distorted and such distortion is also observed in Au_6H_8 and Au_6H_9. However, all the three clusters with the distorted triangular structure are planar. In the Au_6H_7 cluster, migration of two H atoms to an outer Au atom from the nearby Au atoms is observed. Such H atom migration is also observed from the bridge position in Au_6H_8 to the outer Au atom in Au_6H_9. Both bridge bonded H atoms and atoms bonded in the head-on fashion are observed in the three higher clusters. The shortest Au–H bond length for head-on bonded H atoms is 1.55 Å while for the bridge bonded H atoms the Au–H distance is in the range of 1.66–1.79 Å. One of the inner Au–Au bonds is considerably elongated (3.81 Å in Au_6H_7, 3.89 Å in Au_6H_8 and 3.46 Å in Au_6H_9) which is comparable with Au–Au distance in gold nanowires mentioned above. The average bond length of outer Au–Au bonds increase from 2.62 Å in Au_6H_6 to 2.68 Å in Au_6H_9. Elongation of metal–metal bond indicates weakening of the bond which aid in the binding of H atoms. The planarity of the clusters is lost in Au_6H_{10}, Au_6H_{11} and Au_6H_{12} with one of the inner Au atoms protruding out of the plane of the triangle; however the triangular structure of Au_6 is retained. The average Au–Au bond length of the inner Au atoms increases from 2.68 Å in Au_6H_9 to 2.73 Å in Au_6H_{12} and outer Au–Au bond length increases from 2.73 Å in Au_6 to 2.80 Å in Au_6H_{12}. The shortest Au–H distance of the head-on bonded H atom is 1.54 Å and in the range of 1.69–1.78 Å for bridge bonded H atom in the three clusters. Table 2 summarizes the Au–Au and Au–H (both head-on and bridge bonded) distances in Au_6H_n (n = 0–12) clusters.

The binding energy per atom, E_b for the ground states of the Au_6H_n (n = 1–12) clusters is higher than that for pristine Au_6 cluster. This indicates that hydrogen adsorption stabilizes the Au_6 cluster. Both the binding energy per atom and the binding energy per H atom show an odd–even oscillation trend from Au_6H to Au_6H_{12} with the higher value of binding energy for the cluster with even number of H atoms. Thus, the clusters with even number of H atoms possess higher stability compared to the counterparts with odd number of H atoms as evident from the binding energy values. Careful observation of both the energies reveals that the increase in binding energy per atom is prominent till Au_6H_8 while remaining constant with further increase in H-atom and in case of binding energy of per H atom, it again increases till Au_6H_8 (except Au_6H_2) with no further increase in the energy value on subsequent addition of H atoms.

The HOMO–LUMO gap shows a definite odd–even oscillation pattern where clusters with even number of H-atoms possess higher HOMO–LUMO gap. The highest HOMO–LUMO gap of 2.44 eV is observed in Au_6H_8 and addition of H atoms does not increase the gap further. From the HOMO–LUMO gap, it appears that the Au_6 cluster with eight hydrogen atoms is more stable compared to the other congeners. Au_6H_8 also possesses the highest hardness in parity with the highest HOMO–LUMO gap. The value of hardness, η of a cluster is a measure of the reactivity of that particular cluster. Thus, Au_6H_8 will be the least reactive from the perspective of highest η value. Fig. 3 illustrates the HOMO and LUMO orbitals of Au_6, Au_6H_2, Au_6H_4, Au_6H_6, Au_6H_8, $Au6H_{10}$ and Au_6H_{12} clusters. A strong s–d orbital hybridization is seen in the Au_6 cluster evident from Fig. 3. The adsorption of different number of hydrogen atoms changes the electron density of the HOMO and LUMO states. Both the HOMO and LUMO states are mainly localized around the Au atoms along with some amount of distribution around the H-atoms. Distribution around the H-atoms indicates existence of hybridization between the s-orbital of Au and s-orbital of H along with s–d orbital hybridization of Au atoms. Adsorption of H on the inner Au atoms likely results in charge transfer from the HOMO of the Au_6 cluster to the H atom which results in increase in electron

Table 2
Computed selected Au–H and Au–Au bond lengths of Au_6H_n (n = 0–12) clusters.

Cluster	Au–H (Å)		Au–Au (Å)	
	Head-on	Bridge	Outer	Inner
Au_6	–	–	2.59	2.73
Au_6H	1.56	–	2.59	2.74
Au_6H_2	1.73	–	2.59	2.73
Au_6H_3	1.57	–	2.58	2.72
Au_6H_4	1.57	–	2.60	2.72
Au_6H_5	1.56	–	2.60	2.73
Au_6H_6	1.54	–	2.62	2.73
Au_6H_7	1.55	1.66–1.75	2.67	2.78
Au_6H_8	1.55	1.66–1.79	2.67	2.74
Au_6H_9	1.55	1.68–1.75	2.68	2.69
Au_6H_{10}	1.54	1.72–1.78	2.69	2.73
Au_6H_{11}	1.55	1.69–1.76	2.73	2.81
Au_6H_{12}	1.54	1.69–1.77	2.73	2.80

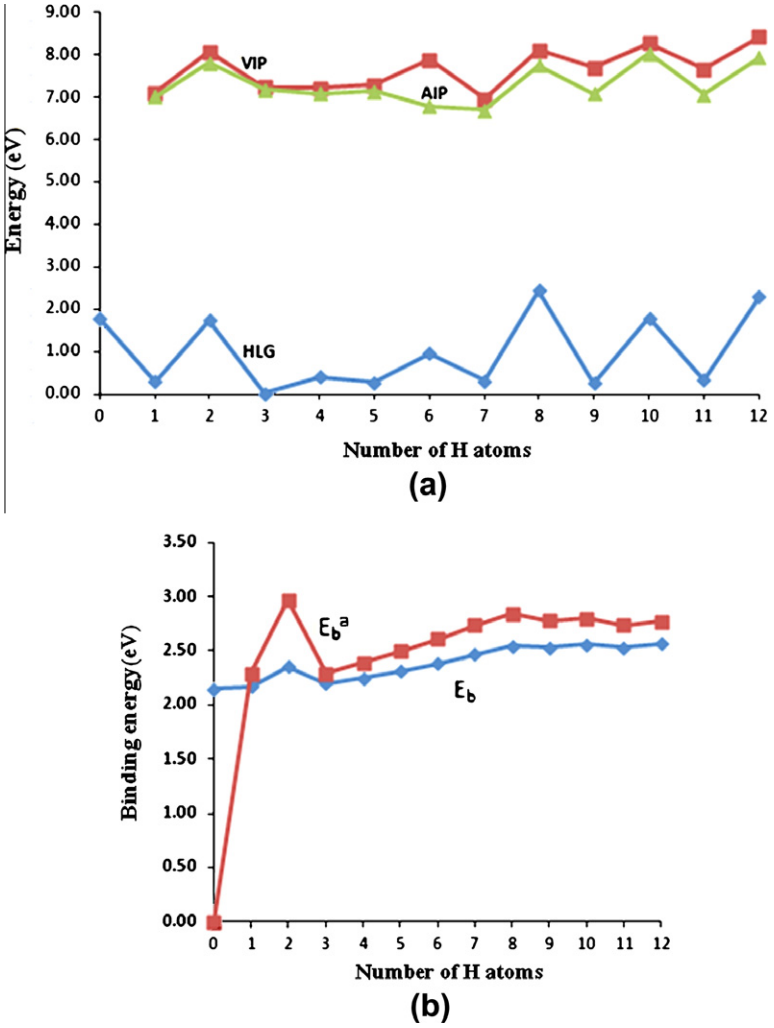

Fig. 2. Variation of (a) vertical ionization potential, adiabatic ionization potential and HOMO–LUMO gap, and (b) binding energy per atom, binding energy per hydrogen atom of the Au_6H_n (n = 1–12) clusters with the number of hydrogen atoms.

density on the later as revealed from the presence of negative charges discussed in the Hirshfeld charge analysis below.

Next, the vertical ionization potential (VIP) and the adiabatic ionization potential (AIP) are considered. The VIP values exhibit an odd–even pattern from Au_6H to Au_6H_3 and then remain constant till Au_6H_5. From Au_6H_6 to Au_6H_{12}, it again exhibits a distinct odd–even oscillation pattern where clusters with even number of H atoms have higher VIP values. Similar odd–even pattern is observed for adiabatic ionization potential values from Au_6H to Au_6H_3 and then remain constant till Au_6H_5. The AIP values decrease in Au_6H_6 and Au_6H_7 while show a definite odd–even oscillation pattern from Au_6H_8 till Au_6H_{12}. The AIP and VIP values indicate Au_6H_2, Au_6H_8, Au_6H_{10} and Au_6H_{12} to be more stable compared to other congeners. Table 3 gives the binding energy per atom, E_b; binding energy per H-atom, E_b^a; vertical ionization potential, VIP; adiabatic ionization potential, AIP; HOMO–LUMO gap, HLG and hardness, η of the Au_6H_n clusters. Fig. 2 shows the variation the above properties with the number of H atoms.

The averaged atomic Hirshfeld charges on H atoms for the Au_6H_n clusters are listed in Table 4. The values indicate that the H atoms are negatively charged and the strong interaction between Au and H atoms results from charge transfers. Analysis of Hirshfeld charges on Au atoms of pristine Au_6 cluster reveal that the inner Au atoms carry equal negative charge while the outer Au atoms are positively charged. Adsorption of H atom on the inner Au atom results in charge transfer from the Au atom to the H atom (see Table 4).

3.2. Fukui function

Analyzing the f^+/f^- and f^-/f^+ values, i.e. the relative electrophilicity and nucleophilicity, respectively of a site in a cluster helps to predict the response of that particular site towards an impending

Table 3
Calculated binding energy per atom E_b; binding energy per hydrogen atom E_b^a; vertical ionization potential VIP; adiabatic ionization potential AIP; HOMO–LUMO gap HLG and hardness η of the Au_6H_n (n = 1–12) clusters.

Cluster	E_b (eV)	E_b^a (eV)	VIP (eV)	AIP (eV)	HLG (eV)	Hardness (eV)
Au_6	2.15	–	–	–	1.77	0.885
Au_6H	2.17	2.29	7.10	7.01	0.29	0.145
Au_6H_2	2.36	2.97	8.06	7.80	1.73	0.865
Au_6H_3	2.20	2.29	7.23	7.17	0.01	0.005
Au_6H_4	2.25	2.39	7.21	7.09	0.41	0.205
Au_6H_5	2.31	2.50	7.29	7.14	0.27	0.135
Au_6H_6	2.38	2.61	7.88	6.78	0.97	0.485
Au_6H_7	2.47	2.73	6.96	6.70	0.30	0.150
Au_6H_8	2.54	2.84	8.11	7.75	2.44	1.220
Au_6H_9	2.53	2.78	7.69	7.08	0.25	0.125
Au_6H_{10}	2.56	2.80	8.28	8.03	1.80	0.900
Au_6H_{11}	2.53	2.74	7.66	7.07	0.33	0.165
Au_6H_{12}	2.56	2.77	8.43	7.93	2.30	1.150

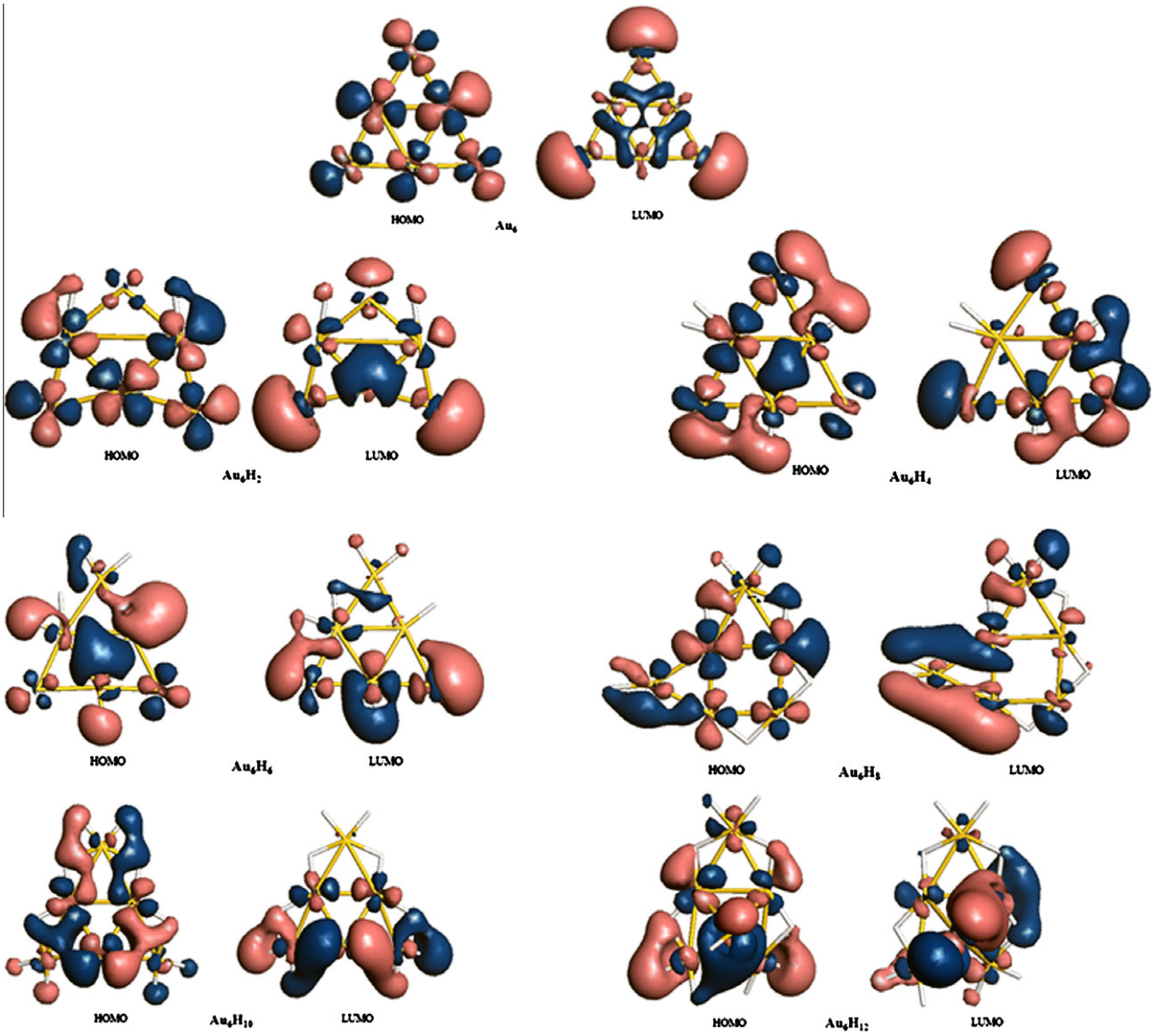

Fig. 3. The HOMO and LUMO orbitals of Au_6, Au_6H_2, Au_6H_4, Au_6H_6, Au_6H_8, Au_6H_{10} and Au_6H_{12} clusters.

Table 4
Averaged atomic Hirshfeld charges on H atom in Au_6H_n (n = 1–12) clusters.

Cluster	Charge
Au_6H	−0.071
Au_6H_2	−0.085
Au_6H_3	−0.094
Au_6H_4	−0.039
Au_6H_5	−0.042
Au_6H_6	−0.059
Au_6H_7	−0.065
Au_6H_8	−0.043
Au_6H_9	−0.060
Au_6H_{10}	−0.052
Au_6H_{11}	−0.053
Au_6H_{12}	−0.049

electrophilic or nucleophilic attack. When we consider the f^+/f^- and f^-/f^+ values for all the six sites present in the Au_6 cluster, we find that on one hand the atoms forming the vertices of the outer triangle have a higher f^+/f^- value while on the other hand, the atoms comprising the vertices of the inner triangle have higher f^-/f^+ value. Thus, the atoms forming the vertices of the outer triangle are prone for a nucleophilic attack like CO and those forming the vertices of the inner triangle are susceptible for an electrophilic attack like O_2. Phala et al. [52] and Wu et al. [61] have also found CO adsorbed on the outer Au atom of neutral Au_6 cluster to be the most stable configuration.

In Au_6H, the Au atom (has higher f^-/f^+ value in pristine Au_6) with adsorbed H atom has the highest f^+/f^- value while the remaining two inner Au atoms still have higher f^-/f^+ value. In Au_6H_2, the higher f^+/f^- value is retained on the outer Au atoms and an inner Au atom with no H adsorbed on it has the highest $^-/f^+$ value. In Au_6H_3 and Au_6H_4, all the Au sites are amphiphilic, i.e. all the six Au atoms possess equal f^+/f^- and f^-/f^+ values. These are likely to donate and withdraw electrons thus, participating in both oxidation and reduction reactions. In Au_6H_6, the reactivity trend of the pristine Au_6 cluster is preserved with one inner Au atom having the highest f^-/f^+ value and a nearby outer Au atom with the highest f^+/f^- value. However, the difference with pristine Au_6 cluster is that in Au_6H_6 specific sites have the highest values unlike having equal values for similar Au sites as in the former. Thus, if we intend to study the CO oxidation on Au_6H_6 cluster, O_2 will adsorb on the inner Au atom while CO on the nearby outer Au atom and will thus serve to be a favorable configuration to investigate the detailed mechanism of the said reaction.

In Au_6H_8, one Au atom forming the vertex of the inner triangle has the highest f^-/f^+ value while another inner Au atom has the highest f^+/f^- value. On the other hand, in Au_6H_{10}, one Au atom forming the vertex of the outer triangle has the highest f^-/f^+ value while another outer Au atom has the highest f^+/f^- value. Thus, in Au_6H_8 both CO and O_2 will adsorb in the vertices of the inner triangle while in Au_6H_{10}, they will adsorb in the outer Au atoms. The reactivity trend of the Au sites in Au_6H_{11} and Au_6H_{12} is however, similar to Au_6H_8. The analysis of the fukui functions indicate the adsorption of H atoms do not alter much the reactivity behavior of Au sites towards an impending electrophile or nucleophile except in situations like Au_6H_8 and Au_6H_{10} where the reactivity trend is changed.

4. Conclusion

The geometric structures, binding energies, HOMO–LUMO gap, chemical hardness and the electrophilicity and nucleophilicity of the Au sites of Au_6H_n (n = 1–12) clusters have been studied at the generalized gradient approximation level using the PBE functional and DNP basis set. The low spin state structures are found to more stable than the high spin counterparts in all the clusters. The high binding energies indicate that the adsorption of H atoms stabilize the Au_6 cluster. The lowest energy structures obtained from the present investigation shows that the structures are planar till Au_6H_9. However, the triangular structure of Au_6 is distorted in Au_6H_7, Au_6H_8 and Au_6H_9. Elongation of Au–Au bond length indicates that the metal hydrogen binding is made at the expense of metal–metal bond weakening. On further addition of H atoms one of the base Au atoms of the Au_6 triangle protrudes out of the plane of Au_6 in Au_6H_{10}, Au_6H_{11} and Au_6H_{12} cluster rendering these clusters non-planarity. The averaged Hirshfeld atomic charges indicate the H atoms to be negatively charged in all the clusters indicating charge transfer from Au to H atoms. Odd–even alternation in HOMO–LUMO gap, chemical hardness, vertical ionization potential, adiabatic ionization potential and binding energy is observed with the clusters having even number of H atoms possessing higher values and are observed to be more stable than their congeners with odd number of H atoms. DFT based reactivity descriptors indicate that in Au_6, the Au atoms forming the vertices of the outer triangle have higher relative electrophilicity value while those forming the vertices of the inner triangle have higher relative nucleophilicity value. This implies that nucleophile such as CO will attack on the outer Au atoms while electrophiles such as O_2 on inner Au atoms. However, in Au_6H_6, two nearby Au sites forming the vertices of the inner and outer triangle have the highest relative electrophilicity and relative nucleophilicity values. In Au_6H_{12}, these are located in the inner triangle.

Acknowledgment

The authors acknowledge the Department of Science and Technology (DST), New Delhi for the financial assistance.

Appendix A. Supplementary material

Supplementary data associated with this article can be found, in the online version, at http://dx.doi.org/10.1016/j.comptc.2012.09.006.

References

[1] P. Pyykko, Theoretical chemistry of gold, Angew. Chem. Int. Ed. 43 (2004) 4412–4456.
[2] M.C. Daniel, D. Astruc, Gold nanoparticles: assembly, supramolecular chemistry, quantum-size-related properties, and applications toward biology, catalysis and nanotechnology, Chem. Rev. 104 (2004) 293–346.
[3] P. Schwerdtfeger, Gold goes nano – from small clusters to low-dimensional assemblies, Angew. Chem. Int. Ed. 43 (2003) 1892–1895.
[4] M. Mavrikakis, P. Stoltze, J.K. Norskov, Making gold less noble, Catal. Lett. 64 (2000) 101–106.
[5] J. Ho, K.M. Ervin, W.C. Lineberger, Photoelectron spectroscopy of metal cluster anions: Cu_n^-, Ag_n^- and Au_n^-, J. Chem. Phys. 93 (1990) 6987–7002.
[6] H. Hakkinen, B. Yoon, U. Landman, X. Li, H.J. Zhai, L.S. Wang, On the electronic and atomic structures of small Au_n^- (n = 4–14) clusters: a photoelectron spectroscopy and density-functional study, J. Phys. Chem. A 107 (2002) 6168–6175.
[7] C.L. Cleveland, U. Landman, T.G. Schaaff, M.N. Shaffigullin, P.W. Stephens, R.L. Whetten, Structural evolution of smaller gold nanocrystals: the truncated decahedral motif, Phys. Rev. Lett. 79 (1997) 1873–1876.
[8] K. Koga, H. Takeo, T. Ikeda, K.I. Ohshima, In situ grazing-incidence x-ray-diffraction and electron-microscopic studies of small gold clusters, Phys. Rev. B 57 (1998) 4053–4062.
[9] C. Jackschath, I. Rabin, W. Schulze, Electron impact ionization potentials of gold and silver clusters Mn, $n \geqslant 22$, Ber. Bunsenges. Phys. Chem. 96 (1992) 1200–1204.
[10] V.A. Spasov, Y. Shi, K.M. Ervin, Time-resolved photodissociation and threshold collision-induced dissociation of anionic gold clusters, Chem. Phys. 262 (2000) 75–91.
[11] B. Palpant, B. Prevel, J. Lerme, E. Cottancin, M. Pellarin, M. Treilleux, A. Perez, J.L. Vialle, M. Broyer, Optical properties of gold clusters in the size range 2–4 nm, Phys. Rev. B 57 (1998) 1963–1970.
[12] K. Balasubramanian, D.W. Liao, Is Au_6 a circular ring, J. Chem. Phys. 94 (1991) 5233–5236.
[13] P.G. Bravo, I.L. Garzon, O. Navarro, Non-additive effects in small gold clusters, Chem. Phys. Lett. 313 (1999) 655–664.
[14] E.M. Fernandez, J.M. Soler, L.C. Balbas, Planar and cagelike structures of gold clusters: density-functional pseudopotential calculations, Phys. Rev. B 73 (2006) 235433.
[15] M.A. Omary, M.A. Rawashdeh- Omary, C.C. Chusuei, J.P. Fackler, P.S. Bagus, Electronic structure studies of six-atom gold clusters, J. Chem. Phys. 114 (2001) 10695–10701.
[16] D.W. Liao, K. Balasubramanian, Electronic-structure of Cu_6, Ag_6, Au_6, and their positive-ions, J. Chem. Phys. 97 (1992) 2548–2552.
[17] P.R. Arratia, L. Hernandez-Acevedo, Spin-orbit effects on heavy metal octahedral clusters, J. Mol. Struct.: Theochem. 282 (1993) 131–141.
[18] O.D. Harberlen, H. Schmidbauer, N. Rosch, Stability of main-group element-centered gold cluster cations, J. Am. Chem. Soc. 116 (1994) 8241–8248.
[19] K. Michaelian, N. Rendon, I.L. Garzon, Structure and energetics of Ni, Ag, and Au nanoclusters, Phys. Rev. B 60 (1990) 2000–2010.
[20] G. Bravo- Perez, I.L. Garzon, O. Novarro, Ab initio study of small gold clusters, J. Mol. Struct.: Theochem. 493 (1999) 225–231.
[21] B.H. Hess, U. Kaldor, Relativistic all-electron coupled-cluster calculations on Au_2 in the framework of the Douglas–Kroll transformation, J. Chem. Phys. 112 (2000) 1809–1813.
[22] H. Gronbeck, W. Andreoni, Gold and platinum microclusters and their anions: comparison of structural and electronic properties, Chem. Phys. 262 (2000) 1–14.
[23] E.M. Fernandez, J.M. Soler, I.L. Garzon, L.C. Balbas, Trends in the structure and bonding of noble metal clusters, Phys. Rev. B 70 (2004) 165403.
[24] Y.D. Kim, M. Fischer, G. Gantefor, Origin of unusual catalytic activities of Au-based catalysts, Chem. Phys. Lett. 377 (2003) 170–176.
[25] K. Sugawara, F. Sobott, A.B. Vakhten, Reactions of gold cluster cations Au_n^+ (n = 1–12) with H_2S and H_2, J. Chem. Phys. 118 (2003) 7808–7816.
[26] J. Wang, G. Wan, J. Zhao, Density-functional study of Au_n (n = 2–20) clusters: lowest energy structures and electronic properties, Phys. Rev. B 66 (2002) 035418.
[27] J. Zhao, J. Yang, J.G. Hou, Theoretical study of small two-dimensional gold clusters, Phys. Rev. B 67 (2003) 085404.
[28] J. Zheng, J.T. Petty, R.M. Dickson, High quantum yield blue emission from water-soluble Au_8 nanodots, J. Am. Chem. Soc. 125 (2003) 7780–7781.
[29] S. Gibb, P. Weis, F. Furche, R. Ahlrichs, M. Kappes, Structures of small gold cluster cations (Au_n^+, $n < 14$): ion mobility measurements versus density functional calculations, J. Chem. Phys. 116 (2002) 4094–4101.
[30] X. Li, B. Kiran, L.F. Cui, L.S. Wang, Magnetic properties in transition-metal-doped gold clusters: M@Au6 (M = Ti, V, and Cr), Phys. Rev. Lett. 95 (2005) 253401.
[31] H. Hakkinen, U. Landman, Gold clusters and their anions, Phys. Rev. B 62 (2002) R2287–R2290.
[32] K.J. Taylor, C.L. Pettite-Hall, C. Cheshmovsky, R.E. Smalley, Ultraviolet photoelectron spectra of coinage metal clusters, J. Chem. Phys. 96 (1992) 3319–3329.
[33] B. Yoon, H. Hakkinen, U. Landman, Interaction of O_2 with gold clusters: molecular and dissociative adsorption, J. Phys. Chem. A 107 (2003) 4066–4071.
[34] W.T. Wallace, R.L. Whetten, Coadsorption of CO and O_2 on selected gold clusters: evidence for efficient room-temperature CO_2 generation, J. Am. Chem. Soc. 124 (2002) 7499–7505.
[35] G. Mills, M.S. Gordon, H. Meitu, Oxygen adsorption on Au clusters and a rough Au (111) surface. The role of surface flatness, electron confinement, excess electrons, and band gap, J. Chem. Phys. 118 (2003) 4198–4205.

[36] H. Hakkinen, M. Moseler, U. Landman, Bonding in Cu, Ag, and Au clusters: relativistic effects, trends, and surprises, Phys. Rev. Lett. 89 (2002) 033401.
[37] F. Furche, R. Ahlrichs, P. Weis, C. Jacob, S. Gibb, T. Bierweller, M.M. Kappes, The structures of small gold cluster anions as determined by a combination of ion mobility measurements and density functional calculations, J. Chem. Phys. 117 (2002) 6982–6990.
[38] W. Huang, L.S. Wang, Probing the 2D to 3D structural transition in gold cluster anions using argon tagging, Phys. Rev. Lett. 102 (2009) 153401.
[39] A.S.K. Hashmi, The catalysis gold rush: new claims, Angew. Chem., Int. Ed. 44 (2005) 6990–6993.
[40] H. Ito, T. Saito, T. Miyahara, C. Zhong, M. Sawamura, Relativistic effects in gold chemistry. I. Diatomic gold compounds, Organometallics 28 (2009) 4829–4840.
[41] C. González-Arellano, A. Corma, M. Iglesias, F. Sánchez, Enantioselective hydrogenation of alkenes and imines by a gold catalyst, Chem. Commun. 27 (2005) 3451–3453.
[42] H. Ito, T. Yajima, J. Tateiwa, A. Hosomi, First gold complex-catalysed selective hydrosilylation of organic compounds, Chem. Commun. 11 (2000) 981–982.
[43] C. Wei, C.-J. Li, A highly efficient three-component coupling of aldehyde, alkyne, and amines via C–H activation catalyzed by gold in water, J. Am. Chem. Soc. 125 (2003) 9584–9585.
[44] M. Conte, H. Miyamura, S. Kobayashi, V. Chechik, Spin trapping of Au–H intermediate in the alcohol oxidation by supported and unsupported gold catalysts, J. Am. Chem. Soc. 131 (2009) 7189–7196.
[45] B. Kiran, X. Li, H.J. Zhai, L.S. Wang, Gold as hydrogen: structural and electronic properties and chemical bonding in $Si_3Au_3^{+/0/-}$ and comparisons to $Si_3H_3^{+/0/-}$, J. Chem. Phys. 125 (2006) 133204.
[46] S. Buckart, G. Gantefor, Y.D. Kim, P. Jena, Anomalous behavior of atomic hydrogen interacting with gold clusters, J. Am. Chem. Soc. 125 (2003) 14205–14209.
[47] P.J. Hay, W.R. Wadt, L.R. Kohn, F.W. Bobrowiez, *Ab initio* studies of AuH, AuCl, HgH and $HgCl_2$ using relativistic effective core potentials, J. Chem. Phys. 69 (1978) 984–997.
[48] P. Schwerdtfeger, M. Dolg, W.H.E. Schwarz, G.A. Bow-maker, P.D.W. Boyd, Relativistic effects in gold chemistry. I. Diatomic gold compounds, J. Chem. Phys. 91 (1989) 1762–1774.
[49] Y. Wang, X.G. Gong, First-principles study of interaction of cluster Au_{32} with CO, H_2 and O_2, J. Chem. Phys. 125 (2006) 124703.
[50] M.G. Guichemerre, G. Chamband, Electronic structure, reactivity, and spectroscopy of dihydrides of group-IB metals, J. Chem. Phys. 122 (2005) 204325.
[51] H.W. Ghebriel, A. Kshirsagar, Adsorption of molecular hydrogen and hydrogen sulfide on Au clusters, J. Chem. Phys. 126 (2007) 244705.
[52] N.S. Phala, G. Klatt, E.V. Steen, A DFT study of hydrogen and carbon monoxide chemisorption onto small gold clusters, Chem. Phys. Lett. 395 (2004) 33–37.
[53] M. Zhang, L.M. He, L.X. Zhao, X.J. Feng, W. Cao, Y.H. Luo, A density functional theory study of the Au_7H_n (n = 1–10) clusters, J. Mol. Struct.: Theochem. 911 (2009) 65–69.
[54] A. Deka, R.C. Deka, Structural and electronic properties of stable Au_n (n = 2–13) clusters: a density functional study, J. Mol. Struct.: Theochem. 870 (2008) 83–93.
[55] B. Delley, An all-electron numerical method for solving the local density functional for polyatomic molecules, J. Chem. Phys. 92 (1990) 508–517.
[56] S.J. Vosko, L. Wilk, M. Nusair, Accurate spin-dependent electron liquid correlation energies for local spin density calculations: a critical analysis, Can. J. Phys. 58 (1980) 1200–1211.
[57] B. Delley, A scattering theoretic approach to scalar relativistic corrections on bonding, Int. J. Quant. Chem. 69 (1998) 423–433.
[58] W. Yang, W.J. Mortier, The use of global and local molecular parameters for the analysis of the gas-phase basicity of amines, J. Am. Chem. Soc. 108 (1986) 5708–5711.
[59] R.K. Roy, S. Krishnamurti, P. Geerlings, S. Pal, Local softness and hardness based reactivity descriptors for predicting intra- and intermolecular reactivity sequences: carbonyl compounds, J. Phys. Chem. A 102 (1998) 3746–3755.
[60] H.-J. Zhai, B. Kiran, L.-S. Wang, Observation of Au_2H-impurity in pure gold clusters and implications for the anomalous Au–Au distances in gold nanowires, J. Chem. Phys. 121 (2004) 8231–8236.
[61] X. Wu, L. Senapati, S.K. Nayak, A. Selloni, M. Hajaligol, A density functional study of carbon monoxide adsorption on small cationic, neutral, and anionic gold clusters, J. Chem. Phys. 117 (2002) 4010–4015.